Journal of Inclusion Phenomena and Molecular Recognition in Chemistry **21**: 299–324, 1995.

Alkali-Metal Clusters as Prototypes for Electron Solvation in Zeolites

NICK P. BLAKE and GALEN D. STUCKY

1. Introduction

In this section we describe, in some detail, work conducted on alkali-metal clusters in zeolites. Almost without exception, the clusters that we will discuss cannot exist in the gas-phase. As we shall demonstrate, the role of the zeolite is to provide an electrostatic containment field which gives rise to certain ionic sites within the zeolite. Alkali-metal ions which, of course, play the role of counter-ion in the aluminosilicate zeolites, only take on the character of a cluster through introduction of an alkali atom or electron to the zeolite. Under these conditions, the electron (either the valence electron of the alkali atom or the introduced electron) is solvated by the electron trap afforded by these counter-ions. The ions relax around the electron and the result is an alkali-metal cluster. The concept is more than merely notional, since many of the physical properties (EPR and absorption cross-section) of the associated electron can be explained in terms of an alkali-metal cluster. Further, circumstantial evidence that the valence electron of an introduced alkali-atom is auto-ionized comes from the fact that XRD reveals that the nucleus takes up one of the ionic sites in the zeolite.

There are a number of reasons why such systems are interesting:

1) Firstly, these clusters, when isolated, are color centers. They may be produced by exposure of the zeolite to γ-rays or UV light and can be bleached by exposure to a high-intensity white-light source. This cathodochromic and photochromic behavior has, in the past, found applications in CRTs and read/write devices [1].
2) Secondly, at higher cluster concentrations, aggregation of clusters leads to new types of materials. These are known to possess different electronic properties, most notably evident in the modified EPR signal and optical absorption spectrum. All of these changes point to the fact that the clusters are coupled and, as such, are highly suitable candidates for the study of metal-insulator transitions. The unique, channel-like structure of the zeolite ensures a highly directional coupling of neighboring clusters found only in these periodic porous structures. The magnetic and electronic properties of these coupled clusters are perhaps the most exciting aspects of the present alkali-metal cluster work.
3) Thirdly, the formation of alkali-metal clusters in photo-induced charge-transfer involving guests within zeolite hosts provides a mechanism for the stabilization of charge-transfer processes. Typically, charge-transfer processes occur at energies

1-4 eV lower than in the gas-phase. In this way, the zeolites exhibit great utility in the formation of new chemical species and stabilization of charge-separated intermediates. As we shall see, this may lead to selectivity in photo-oxidation reactions.

4) A full, quantitative understanding of the physical properties of these clusters is an indirect way of probing the all-important electrostatic fields within the cages and channels of the zeolites. This fundamental property of the zeolites is essential in the modeling of thermodynamic and transport processes; furthermore, with minor modifications, ab initio packages can be used to model electronic changes in guest molecules and introduction into the zeolite, as well as modifications in the magnetic properties of the system.

2. Methods for the Preparation of Alkali-metal Clusters.

To date, a great many alkali-metal clusters have been identified. Table 1 shows some of the alkali-metal clusters that involve exclusively Na; while in Figure 1, we show the structures of these zeolites and how they are related to the cubo-octahedral sodalite cage. The type of cluster observed, to a large extent, depends upon the method of preparation. We now discuss the primary techniques employed.

2.1 EXPOSURE OF THE ZEOLITE TO HIGH-ENERGY RADIATION

This technique is discussed first for historical reasons. In 1965, Kasai [2] found electron-capture induced through exposure of Na-Y to γ-radiation led to the formation of Na_4^{3+} color centers. Typically, in such studies, the zeolite sample is pressed into a semi-transparent disc which normally requires pressures of 5000 lb/in^2. In the case where the zeolite to be studied is dehydrated, it is necessary to mount the disc in a vacuum apparatus (10^{-3} Torr) and dehydrate at elevated temperatures (200-300° C) for periods of several hours. This disc can then be exposed to either a pulsed high-energy electron beam (10^6 rad/pulse, 2 ns pulse duration) [3] or if steady-state measurements are required, a ^{60}Co γ-ray source of dosage rates of 9.5 krad/min is sufficient.

In cathodochromic studies, air-sensitive zeolites are undesirable and so typically halo-sodalites are preferred. These can be prepared using traditional solid-state synthetic methods (make a gel of $NaAlO_2$, SiO_2, and NaBr in water and evaporate to dryness); however, to improve the cathodochromic properties of the solid, it is found that it is best to 'fire' the product for a few hours at temperatures of around 1000° C. The reasons as to why this procedure is required will become evident later. The resultant powder may then be deposited on an aluminum substrate to a thickness of 0.5 mm or for CRT applications, the powder may be settled in a water suspension and processed according to standard CRT manufacturing methods [1]. Coloration of the samples is effected using electron

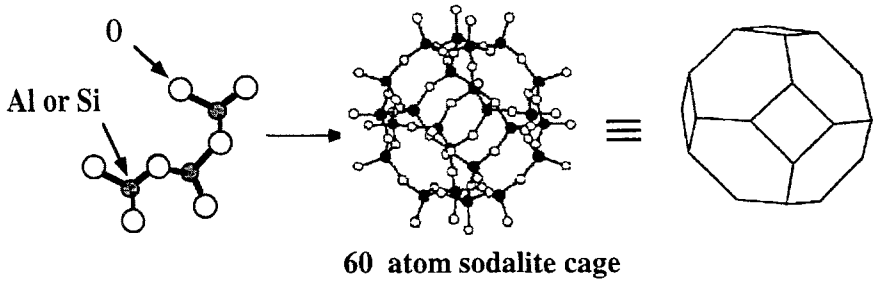

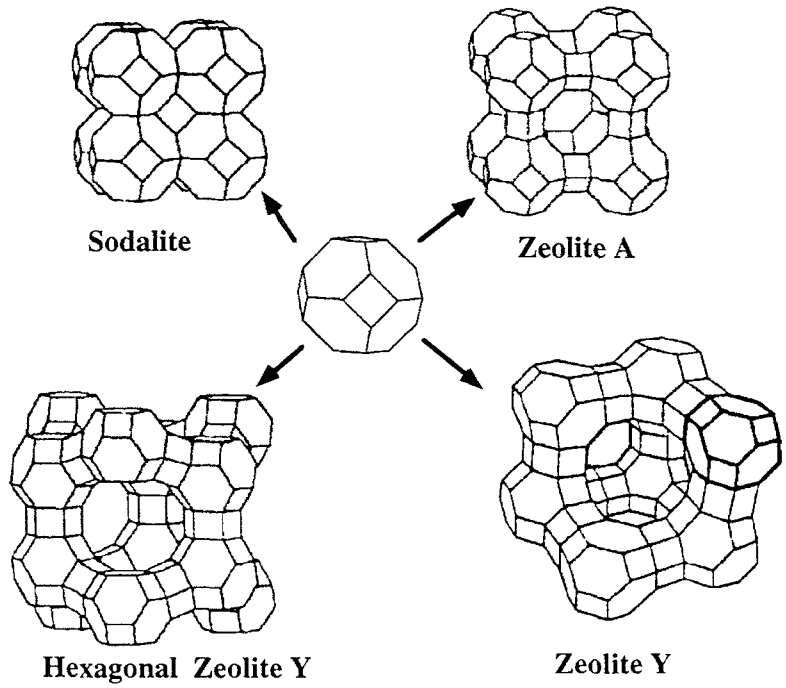

Figure 1. Structures of zeolites sodalite, Na-A, and Na-Y.

Table 1. Na_{n+1}^{n+} observed to date and method of formation.

Cluster	Zeolite	Method of formation	Reference
Na_2^+	Na-A	electron capture 77 K	[3]
Na_3^{2+}	Na-Y	organolithium reagents	[4]
	Na-A	electron capture 196 K	[3]
	Sod	electron capture 196 K	[5]
Na_4^{3+}	Na-Y	electron capture	[2]
		organolithium reagents	[4a]
	Sod	Na-doping	[6,7]
		Na-doping halo-sodalites	[8]
		electron capture in halosodalites	[1]
	Na-Y	Europium metal exchange in liquid NH_3	[9]
	Na-X	electron capture	[3]
		organolithium reagents	[4a]
Na_5^{4+}	Na-X	Na-doping	[4b]
Na_6^{5+}	Na-X	Na-doping	[4b]

energies of 5-20 keV - standard in CRT applications. Generally speaking, higher sensitivity and contrast ratios are obtained with the higher energy electron beams. The charge densities employed can be varied from 0.01-100 mC/cm^2. The number of color centers produced per electron has been estimated at around 100. Bleaching can be achieved using an unattenuated white-light source with illumination intensities of around 10,000 lx, where it is found that bleaching to half the initial value typically takes 15 sec. The bleaching time is found to be inversely proportional to the light intensity and occurs with quantum efficiencies of 1% or so. It is also found that samples prepared with higher energy electron beams have longer bleach times owing to the larger penetration depth of the electron-beam itself. At room temperature dark, thermal bleaching may take up to several days.

Such techniques, generally speaking, are good for producing isolated clusters and the types of clusters produced are limited. In halo-sodalites, EPR reveals that the color center produced is M_4^{3+} where M is one of the alkali-metals, normally Na. By varying the nature of the host sodalite, it is possible to vary the color of the alkali cluster. Empirically for the sodalites it is found that the wavelength of the absorption maximum is proportional to the lattice constant of the host - this is discussed in more detail in the penultimate section. In Na-X and Na-Y, it is found that the only color center produced is

Na_4^{3+}. In Na-A, at liquid nitrogen temperatures, EPR reveals that the preferred trapping site is Na_2^+ while at 196 K, Na_3^{2+} is the preferred site.

In dehydrated sodalite, the situation is more interesting however. The diffuse reflectance spectrum for the γ-irradiated sodalite gives two overlapping features of comparable intensity, one at 680 nm and the other at 550 nm. The distinct chemical identity of each absorption feature is confirmed by measuring the quenching of each feature in the presence of O_2. The assignment of these features comes from a comparison to the more unambiguous results for Na-A and Na-X where it is known that at 196 K irradiation gives Na_3^{2+} and Na_4^{3+}, respectively. Since Na-A has only one electronic feature centered around 650 nm and Na-X one feature at 560 nm, the two features in sodalite are attributed to Na_3^{2+} and Na_4^{3+}, respectively. Figure 2 shows the EPR signal of the γ-irradiated sodalite taken from [5]. The 10-line signal characteristic of Na_3^{2+} is clearly evident. It is, however, perplexing that the 13-line Na_4^{3+} signal is not *more* evident.

On the strength of the O_2 quenching data alone, Thomas et al. [11] have speculated that the Na_4^{3+} center in Na-A resides in the β-cage while the Na_3^{2+} must be produced in an α-cage. This conclusion arises from the premise that electron species in sodalite cages cannot be quenched by O_2 owing to the small pore size. If this conclusion is correct, it is

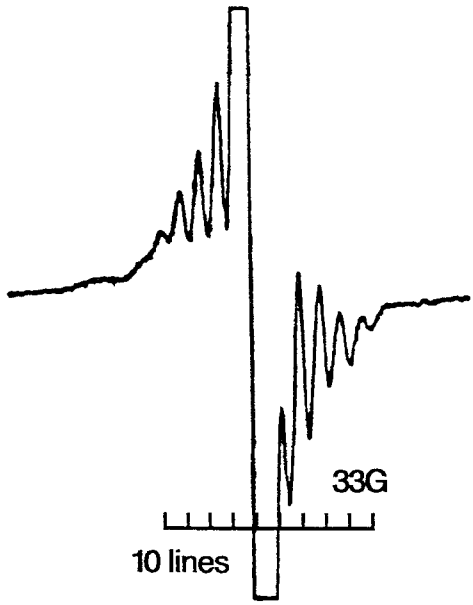

Figure 2. The observed EPR spectrum of the color center obtained upon irradiation of dehydrated sodalite at 196 K (taken from [5]).

puzzling that Na_3^{2+} exhibits the same absorption spectrum in both Na-A and sodalite. As we shall show in the theory section, the absorption spectrum for the color centers is *extremely* sensitive to the dimensions of the cluster; thus the fact that the Na_3^{2+} clusters absorb in the same spectral region in both Na-A and sodalite is more indicative that the species is present in the sodalite cage in both cases. In this case, it may be that the resilience of Na_4^{3+} to quenching is more a result of the fact that most windows into the sodalite cage are occupied by Na^+ ions themselves so that O_2 is unable to gain access to the cage. Bearing all this in mind, the inordinately larger quenching rate observed in Na-A may be simply a transport effect owing to the higher diffusion rates through the solid, coupled with the fact that the ionic sites within the sodalite cage accessible from the α-cage are not occupied by Na^+ ions; however, such an explanation cannot account for the fact that Na_2^+ is not quenched by O_2 .

In addition to the exposure of the zeolite to X-rays, one can, by exposing the zeolite to UV light with energies in excess of 5 eV, ionize the zeolite itself. These electrons are thought to originate from the valence band of the zeolite which Barr et al. report is comprised of the non-bonding O(2p) orbitals [10]. The electrons thus generated are then trapped at cationic sites with the subsequent formation of alkali-metal clusters [11]. Thomas et al. studied Na-X, Na-Y, Na-A, and sodalite after exposure to either 193 nm (6.4 eV) or 185 nm (6.7 eV) light. As with the studies conducted with γ-irradiated zeolites, they found that the same alkali-metal clusters are formed although the intensities are much weaker for UV generated electrons. This is to be expected, since each UV photon absorbed will produce one electron and hence one color center, whereas a γ-ray electron may produce 100 centers.

2.2 ALKALI-METAL DOPING

Shortly after the founding work of Kasai on γ-ray irradiated Na-Y, Kasai, Rabo, and co-workers [12] reported that exposure of Na-Y to Na vapor in vacuo acquired a bright red color attributable to the very same Na_4^{3+} color center. When exposed to Na vapor under the same conditions, Na-X, with its higher Na^+ content, produced a blue color which was interpreted in terms of the cluster Na_6^{5+}. However, EPR evidence was inconclusive and spectra with between 16-19 lines were observed; furthermore, the individual lines did not correspond to a binomial distribution. It was not until the work of Anderson and Edwards, in 1991 [4b], that this problem was resolved. They found that they could simulate the observed EPR spectra with almost equal admixtures of Na_5^{4+} and Na_6^{5+}, see Figure 3.

Thus, the introduction of additional alkali-metal atoms into the zeolite led to the formation of some different 'ion-rich' clusters not seen in the irradiated zeolites. Furthermore, through doping with different alkali-metal ions, it is possible to generate analogs of the Na clusters observed in the previous section. Edwards and co-workers have been able to elucidate the existence of three further centers - K_4^{3+} [13], K_3^{2+} (in K-A and K-X) [4c], and Na_3^{2+}, [4a] in zeolites X, Y, and A.

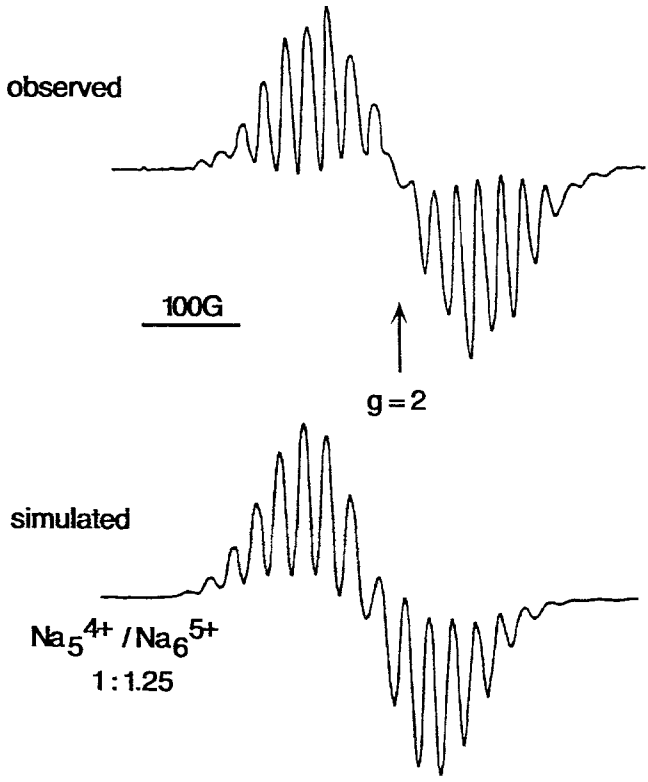

Figure 3. The top figure is the first derivative of the EPR spectrum obtained when Na-X is doped with Na at 298 K. The lower figure is the simulated spectrum for a mixture of the Na_5^{4+} and Na_6^{5+} color centers in the ratio 1:1.25 (taken from [4c]).

The doping amount can be controlled using methods outlined by Dye [14] whereby the alkali-metal is distilled into calibrated lengths of capillary. Doping in this way can have setbacks however. Generally, it is found that the initial reaction of the zeolite with the vapor is not uniform owing to the fact that certain regions of the zeolite have less of their surface exposed. Homogeneity can be achieved by annealing and frequent rotation of the reaction vessel. Owing to air sensitivity, it is necessary to keep the reaction chamber sealed at all times and, thus, EPR and NMR measurements must be performed in a spectrosil section of the reaction tube. Whilst reaction is most easily effected at higher temperatures, poorer crystallinity is the result. Anderson and Edwards have thus suggested that the best crystallinity is obtained at temperatures as low as 250° C (300° C for Na-A) with annealing times of several days. Combining these techniques, it is possible to obtain homogeneous samples of uniform color.

Doping has an additional feature that makes this method important: notably that much higher concentrations of clusters can be produced. This property distinguishes the zeolite systems from other materials in which color centers can be generated - the most well known being alkali-halide crystals. In these systems, the number of color centers that can be created is restricted by the number of defect sites inherently present in the material. In zeolites, the number of color centers is determined by how many of the zeolite cavities have available ionic sites. In the case of dehydrated sodalite, for example, Barrer showed that the crystal was capable of sorbing sufficient Na atoms such that an alkali-metal cluster was formed in each cage [6]. In addition, a gradual darkening accompanies continued sorption indicating that the electronic properties of the solid change with doping. This feature is present in all zeolites; thus, exposure of Na-Y to low concentrations of alkali-metal changes the sample from white to pink. Continued exposure then turns the sample red, which EPR shows is due to Na_4^{3+}, through purple to black. The EPR spectrum of the material also changes with increasing dopant concentrations, leading to an eclipse of 13-line Na_4^{3+} feature by a narrow singlet. Anderson and Edwards show that this singlet is also present in highly doped Na-A and Na-X, while Barrer [6] and Srdanov, Stucky, and co-workers [7] (see Figure 4) have revealed its presence in fully doped dehydrated sodalite.

The fact that this singlet is evidenced in sodalite clearly suggests that its origin is somehow linked to coupling of Na_4^{3+} centers. In Na-X, Na-Y, and Na-A, the singlet may be due to the coupling of other such color centers. This issue has been meticulously investigated by Anderson and Edwards [15]. Figure 5 shows how the EPR signal changes upon increasing the number of Na atoms per unit cell. All structure attributable to the Na_4^{3+} color center gradually becomes eclipsed by a singlet signal. Anderson and Edwards found that *the singlet signal becomes important at concentrations as low as 3 additional Na atoms per unit cell where the probability that two neighboring cages both possess* Na_4^{3+} *centers becomes significant.* When 8 additional atoms are added, all

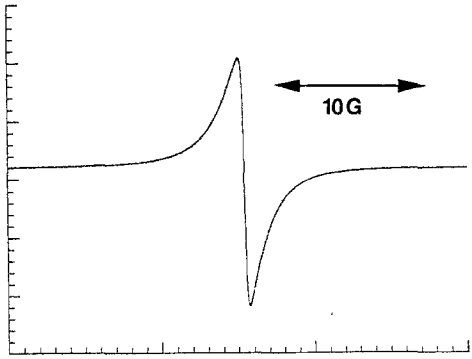

Figure 4. First derivative EPR signal observed in the fully Na-doped system (reproduced by kind permission of Dr. V. I. Srdanov).

β-cage sites are occupied and the singlet eclipses the multiplet structure. This observation adds force to the conclusion that the singlet signal is a result of coupling color centers.

One complication that arises in the cases of Na-Y, Na-X, and Na-A is that exposure to high concentrations of Na leads to a gradual destruction of the crystallinity of the solid. Thus, even though in Na-Y up to 150 Na atoms can be sorbed per unit cell, damage to the framework is observed with concentrations equivalent to 50-60 atoms per unit cell; in Na-X, this threshold is 40-50 atoms per unit cell, while in Na-A damage to the crystallinity is observed at all doping levels.

The K variants of the Na clusters can be prepared by K doping of K-exchanged zeolites. At low doping amounts, and at low temperatures (77 K), K_3^{2+} is the preferred trapping site [4c] in both K-A and K-X; both lead to the characteristic 10-line EPR signals with

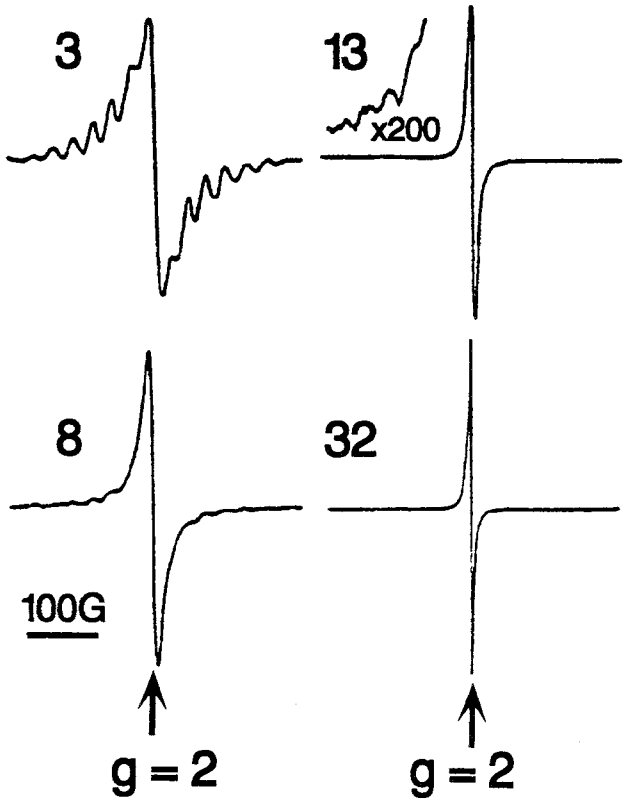

Figure 5. Dependence of the EPR signal of Na/Na_{55}-Y for 3, 8, 13 and 32 additional Na atoms per unit cell (taken from [15]).

hyperfine coupling constants of 12.8 G. This can be viewed as evidence that the cluster must reside in the sodalite cage in both systems. It is unclear whether loss of hyperfine coupling at higher temperatures occurs because of thermal instability or motional averaging.

Sun and Seff [16] recently reported a single crystal XRD study of $K_{12.5}$-A. They found that the occupancy of the sodalite cages in the crystal increases from 1.5 to 2.5 on doping with K vapor and a concomitant K-O bond length increase on K sorption from 2.6 Å to 2.8 Å. The K ions are thus recessed further inside the sodalite cavity. The formation of K_3^{2+} inside the sodalite cavity is thus supported by both XRD and EPR. Furthermore, it is consistent with the work of Thomas' group on cluster formation in dehydrated sodalite and dehydrated Na-A where the similarity in the UV-Vis spectra attributable to Na_3^{2+} suggests that the species both originate within the sodalite cavity.

More recently Armstrong, Anderson, and Edwards [17] have analyzed the K-A system at higher doping levels using XRD. In the K_1/K_{12}-A doping regime, the solid turned an intense blue color. Results from XRD suggest that the K preferentially enters the sodalite cage in the so-called K3 site. They found that the thermal parameters for occupation of the possible ionic sites decreased, suggesting that tumbling motion present in the empty K_{12}-A had ceased. However, while we have the correct stoichiometry to form a K_4^{3+} in the sodalite cage, XRD shows this not to be the case. This led Edwards and co-workers to suggest that the electron density must reside in the α-cage (in seeming contradiction to Anderson and Edwards' earlier work [4c]). In the K_3/K_{12}-A and K_5/K_{12}-A doping regimes, the color of the samples changed through brown to green. In addition, they found evidence for the existence of supercell structure arising as a result of K ordering in neighboring α-cages. The ionic sites K1, K3, and K4 refined to values of 0.5 which turns out can be rationalized through proximity arguments alone. Thus, neighboring K3 and K1 sites are too close to one another to be simultaneously occupied, as are K1 and K4 sites which are only 3.3 Å apart. To overcome this possible source of instability, alternate α-cages either contain 8 K1 or 12 K4 sites leading to a supercell consisting of two conventional zeolite A unit cells. Unfortunately, however, the location of the electrons remains a mystery, since no hyperfine structure is detected in the EPR spectrum down to 77 K.

It is, perhaps, rather surprising that the halo-sodalites can be doped with alkali-metal atoms. Nonetheless Na, K, Cs, and Rb can all be sorbed [8] despite the fact that in the perfect crystal no ionic sites remain for sorbed alkali atoms. However, NMR studies of Stucky et al. [18], clearly show that the conventional synthetic procedures for the production of the halo-sodalites leads to dehydrated sodalite cage 'defect sites'. Later DORS NMR studies by Jelinek, Chmelka, Stein, and Ozin [19] indicated that 10% of the sodalite cages were dry-defect sites. Thus, alkali-metal doping must proceed through uptake into defect cages, where the color centers are created - similarly the production of the color centers in the irradiated halo-sodalites must initially occur through trapping at the dry defect sites, as observed in the work of Thomas' group, followed by ion migration to the cluster site. Smeulders et al. [8] studied the effects of alkali-metal (Li, Na, K, Rb, and Cs) doping in the chloro-, bromo-, and iodo-sodalites. The EPR results obtained

suggested that, in all cases, the Na_4^{3+} color center was formed. This result suggests one of three things:

1) The Na_4^{3+} cluster is more stable in the halo-sodalites of type $Na_4[AlSiO_4^-]_3X_2$ than the possible mixed-ion clusters. This certainly makes sense for the K, Cs, and Rb experiments where their electron affinities are lower. It would not necessarily explain the Li results; however, Li is known to be anomalous in many such situations.
2) If the mixed-ion clusters were of comparable stability to the Na cluster, then the result may be due to Na ion transport. If, for example, we have a cluster Na_3K^{3+}, then even if K and Na ions have equal diffusion rates through the zeolite (in fact, it is most probable that Na has a higher diffusion rate than K ion), it is 3 times as likely that a Na ion will leave as a K ion. When the ion leaves, it will take the electron with it leaving a Na_4^{3+} cluster with a K ion in a neighboring 'empty cage'. Thus, if the observations of the Smeulders group are correct, then both thermodynamic and kinetic effects may be responsible for the exclusive formation of Na_4^{3+} clusters. The third possibility takes another tack:

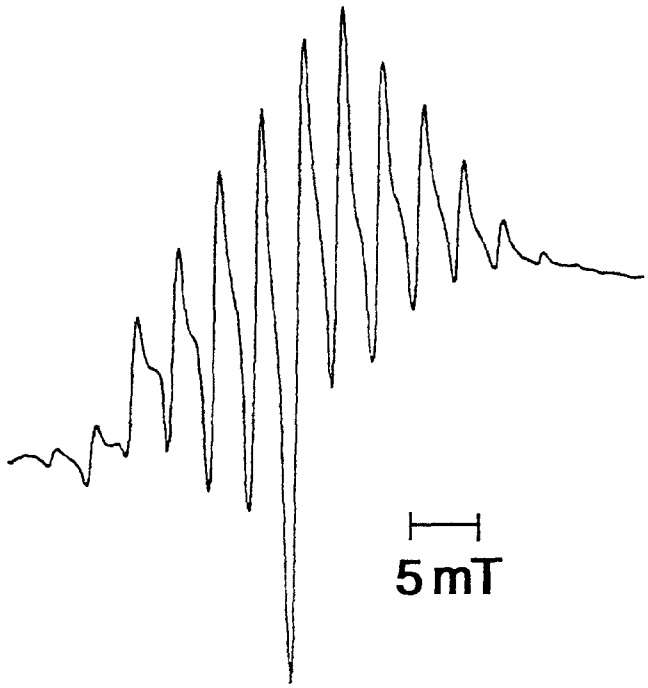

Figure 6. Observed EPR spectrum of Li-doped $Na_4[AlSiO_4]_3Cl$ [8].

3) Mixed ion clusters do exist but could not be discerned in the EPR spectrum. This last alternative is given credence by virtue of the fact that in some cases, i.e., Li/Cl-sodalite (see Figure 6), and Cs/Cl-sodalite systems, non-binomial distributions of the multiplets are observed. This observation is usually synonymous with multiple clusters being present. Furthermore, some of the multiplet lines exhibit shoulders suggesting hidden features in the spectrum.

It seems likely that the behavior of the heavier alkali-metals in such systems may be quite different - as one sees a decrease in the ionicity of the guests. These systems are generally prepared first by ion-exchange, followed by doping with the alkali-metal vapor. Seff and co-workers [20], for example, report the existence of linear Rb_4^{3+}, Cs_3^{2+}, and Cs_4^{3+} clusters along with a triangular Rb_3^{+} cluster in sodalite cages of zeolite-A. XRD of $Rb_{14}[AlSiO_4]_{12}$ [21] reveals that a cluster of the type Rb_6^{4+} may exist. This species involves 3 Rb ions in the sodalite cage connected to a further 3 Rb ions in the supercage connected via the six-ring window. Similar clusters have also been seen in $Rb_{12}Ag_x$-A (x=3,7) [22].

2.3 INTRODUCTION OF MOLECULAR ELECTRON DONORS

2.3.1 Photo-Induced Electron Donors

The idea is simple, introduce into the zeolite some molecule that can donate electrons to the zeolite. The method has conceptual similarities to the cathodochromic work of the first section. The essential distinction is that the electron is 'injected' without creation of structural defects within the zeolite. All of the work discussed here involves electron donation through photon absorption by the guest. Thomas and co-workers at Notre Dame have studied the photoionization of the arenes - pyrene and anthracene sorbed in Na-Y and Na-X [23]. Again, the primary color center produced is the Na_4^{3+} and studies have to be limited to zeolites large enough to accommodate the guest.

2.3.2 Reducing Agents

Use of reducing agents may be considered as an alternative to that of doping the zeolite with the alkali-metal vapor. One class of reducing agent that has found favor is the solvated electron mixtures. The first to be reported involved exposure of Na-X to Eu in liquid NH_3 [9]. Other such mixtures include Li/primary amines [4a] and M/THF (M = alkali-metal) [24]. Alternatively, one can impregnate the zeolite with an alcoholic mixture of the corresponding alkali-metal azide followed by thermal decomposition [25] or directly mix the zeolite with the pertinent alkali-metal azide and thermally decompose [26].

3. Spectroscopic Properties of Alkali-metal Clusters and What They Tell Us About Them

3.1 STUDIES OF ISOLATED ALKALI-METAL (F-CENTER) CLUSTERS

3.1.1 Electron Paramagnetic Resonance

From the bulk of the work discussed above, it is clear that the main technique used in the identification of the type of cluster present has been EPR. At low cluster densities and low temperatures, the electron is observed to couple with the spin $^3/_2$ alkali-metal nuclei of the cluster. It does this democratically, i.e., all nuclei are seen as equivalent to the electron leading to 3N+1 lines with a binomial intensity distribution. This has led workers to the notion of an alkali-metal cluster with an electron 'solvated' in the field supplied by the alkali ions themselves either in simple 'electrons-in-a-box' models [3,6] or more sophisticated one-electron models [3,7,27,28]. In addition, the hyperfine coupling constants are characteristically small, becoming smaller with size of cluster. Since the hyperfine coupling gives information regarding the electron density at the nuclei themselves (i.e., the degree of S character of the valence electron), this indicates that the larger the cluster, the more delocalised the electron - again consistent with the picture of an electron solvated in the ionic-field of the cluster. For the Na_4^{3+} cluster for example, it is estimated that the spin-density at each nucleus is around 10% of that of the valence electron in Na, while in Na_6^{5+} the spin density is estimated at only 7.5%. In both cases, these figures are less than the 100%/N expected for an electron residing in the valence orbital of the free atom and therefore suggests that the electron occupies the space *between* the ions. These arguments are equally valid for the K clusters as well, thus, for K_3^{2+}, for example, the spin density is 16% of the free atom. In the case of the Na_4^{3+} color center, further spectroscopic evidence points to the fact that the cluster is tetrahedral and subject to a central forcefield. This comes from the only Raman study of the cluster reported to date by Sen et al. [29]. They find the characteristic normal modes A, E, and T_2 for the cluster with the correct intensity ratios expected for a tetrahedral cluster subject to a central forcefield - adding weight to the interpretation of an electron delocalised in the space between the ions of the cluster. In cases where several types of cluster are present, interpretation of EPR becomes difficult without modeling of the data. Unfortunately, all clusters exhibit similar hyperfine coupling constants and, as such, the observed spectrum may be a complicated superposition of signals. The best example is that of the Na-doped Na-X work of Anderson and Edwards discussed in the previous section. The hallmarks for admixtures of different clusters appear to be i) non-binomial intensity ratios and ii) non-constant numbered multiplet features from sample to sample.

3.1.2 Optical Properties of the F-centers

In addition to the EPR data, perhaps the second most extensively used technique for characterization has been electronic absorption spectroscopy. This seems natural considering that these clusters are also color centers. In all cases, the absorption bands are broad and featureless containing no vibronic structure. Thus, obtaining any structural information from this technique is difficult without comparison to theoretical calculation. However, in principle, this method reveals information not only about the ground electronic state but also the excited electronic surfaces, which in turn contain information regarding the electrostatic fields inside the zeolite. This led Haug, Srdanov, Stucky, and Metiu [7,27] and later Blake, Srdanov, Stucky, and Metiu [28] to use 3-d wavepacket calculations for the simulation of the electronic absorption spectrum for an electron solvated in the Coulombic field supplied by the sodalite. In this model, a pseudo-potential description of the electron-frame interaction was used. In the first papers by Haug and co-workers, a Shaw-type pseudo-potential description was used. The sensitivity of the obtained spectrum to both charges of the framework atoms and the tetrahedral radius of the color center were investigated. They found, in all charge schemes, that the electron did delocalize at the center of the alkali cluster in the electronic ground state and that the spectrum was mostly sensitive to the tetrahedral radius of the cluster. With this in mind, later calculations by Blake et al. included calibration of a Born-Mayer Na^+-ion framework potential:

$$V_{Na\text{-}ion}(r) = A_{ion} \exp(-r/\rho_{ion}) + Q_{Na}Q_{ion}/r \quad (1)$$

where Q_{ion} is the partial charge assigned to a given framework atom. In addition, an improved pseudo-potential based on the notion of Gaussian charge distribution was adopted:

$$V_{electron\text{-}ion}(r) = - Q_{ion}\, \mathrm{erf}(r/2^{1/2}\Delta_{ion})/r \quad (2)$$

where Δ_{ion} is the crystal radius of the atom as catalogued by Shannon [30]. The parameters that describe these potentials are given in Table 2.

Using this approach, both Na-ion positions and the electronic ground-state energy were minimized. These calculations were successful in reproducing the absorption spectra of not only the Na-doped sodalite but also all of the color center spectra in the halo-sodalites (Figure 7). The model successfully predicts the apparent linear relationship observed in the wavelength of the absorption maxima vs. lattice constant of the sodalite host (Figure 8) while the calculated distance for the nearest Na-ion neighbors to the color center agree to within 0.02 Å with those inferred from the EPR work of Smeulders and co-workers (Table 3). Thus, indicating that a picture of electron solvation within the sodalite is consistent with the observed absorption spectra for the color centers in sodalites. In the

Table 2. Parameters that define the electron-sodalite pseudo-potential and the Na-framework forcefield.

Atom	A (eV)	ρ (Å)	Q (e)	$2^{1/2}\Delta$ (Å)
Na	0	0	+1.0	1.65
O	1224.5	0.284	-0.7	0.82
Si	0	0	+1.0	0.75
Al	0	0	+0.8	0.57
Cl	1551.7	0.334	-1.0	2.56
Br	1594.6	0.347	-1.0	2.77
I	1595.4	0.373	-1.0	3.10

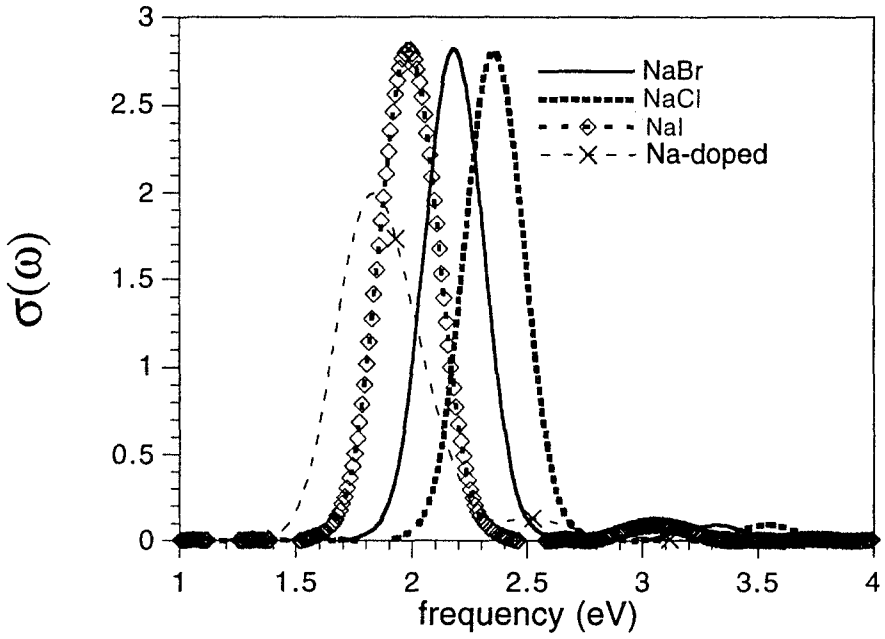

Figure 7. Calculated absorption spectra for the Na_4^{3+} color center in various sodalite hosts.

Table 3. Radial displacement of the Na-ions from the cage center. The values given in parentheses for shell 1 are those for the crystalline host.

Host Lattice	Shell 1 (Å)	Shell 2 (Å)
dry sodalite	3.32 (3.71)	4.14
Cl-sodalite	2.61 (2.73)	4.97
Br-sodalite	2.73 (2.88)	4.89
I-sodalite	2.89 (3.12)	4.72

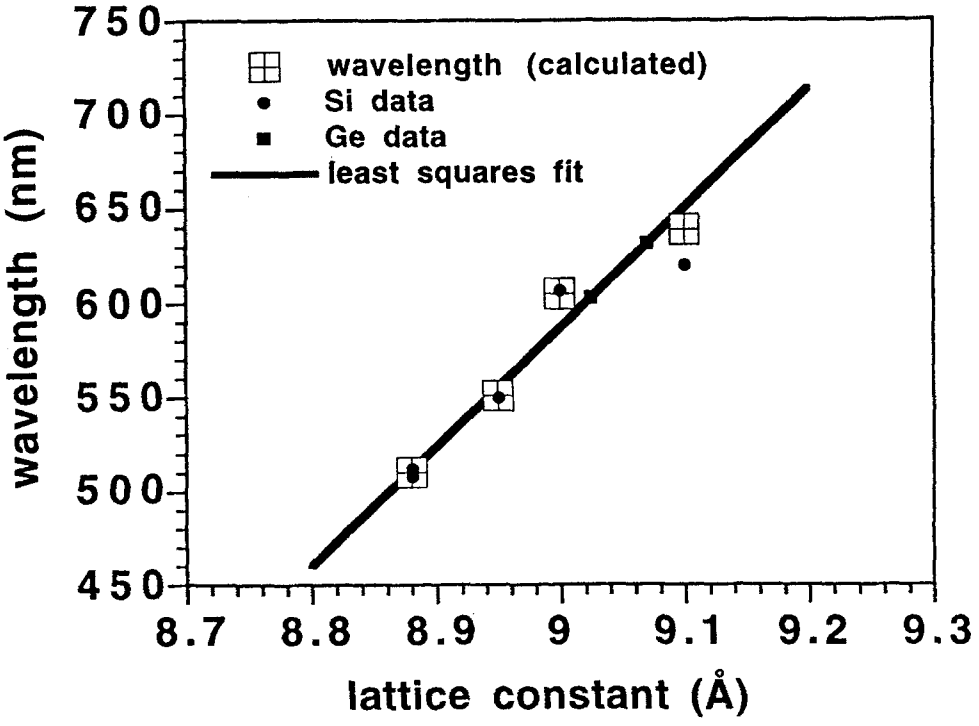

Figure 8. A plot of both the experimentally and theoretically determined wavelengths of maximum absorption for the Na_4^{3+} color center as a function of the lattice constant of the sodalite host.

ground state, the electron does indeed delocalize around the center of the alkali-metal cluster (Figure 9) in the space between the ions. This is in accord with the interpretations from the EPR coupling constants and confirms the geometry of a perfect tetrahedral cluster (in agreement with the Raman spectrum). The electronic states accessed through photon absorption are characterized by their t_2 symmetry (triply degenerate irreducible representation of the T_d point group) with two lobes (one of positive phase and the other negative) pointing along the *{100}* axes (Figure 10). The node is located at the center of the cluster, thus ensuring orthogonality with the ground state (Figure 9). On optical excitation, the resultant deshielding of the ions from one another forces the Na-ions into motion and an effective breathing of the cluster [31]. In part, it is this motion that leads to the broad absorption profile. Recent calculations by us suggest that this motion in itself is not enough to explain the width observed in experiment for the halo-sodalites. Widths of the order of 0.15 eV FWHM are expected while widths from single crystal work are of the order 0.3 eV. It is therefore likely that both inhomogeneity (maybe coupling with the electron hole in the cathodochromic work) and coupling with O is important in determining the final width.

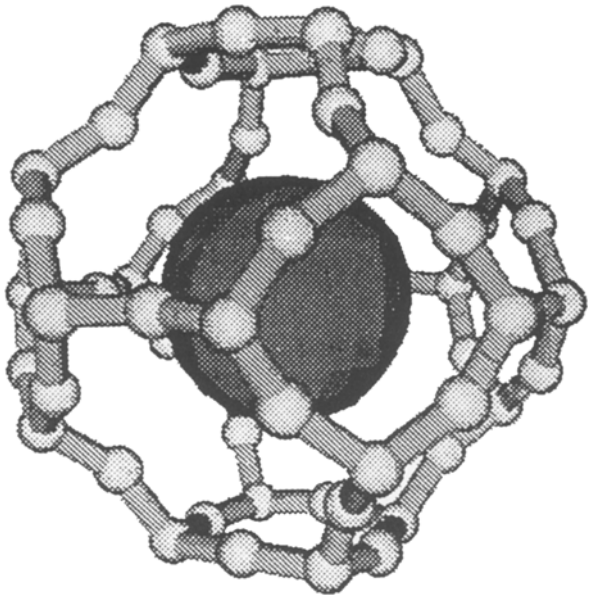

Figure 9. A plot of the electron density for the solvated electron in the ground electronic state in the Na-doped chloro-sodalite ($Na_4[AlSiO_4]_3Cl$).

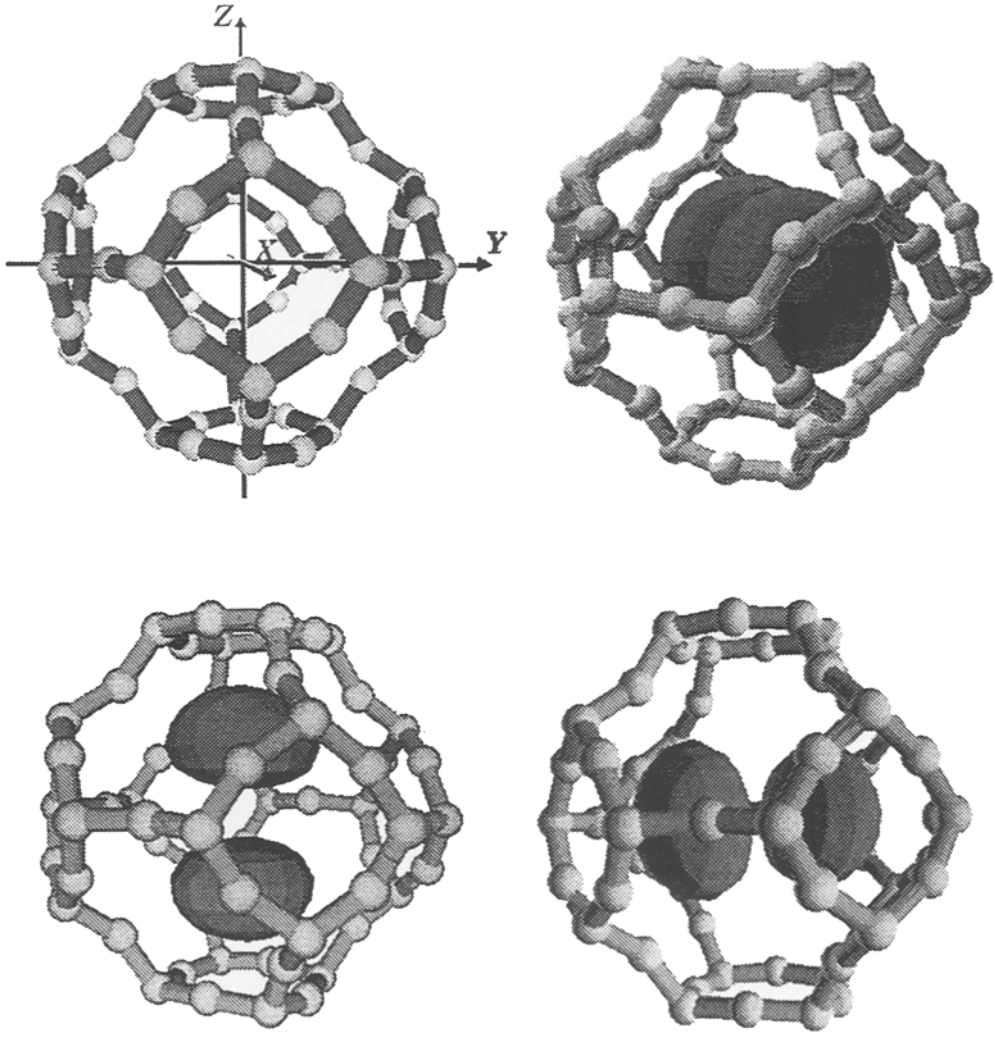

Figure 10. Plots of the electron density for the solvated electron in the first excited, triply degenerate t_2 states in the Na-doped chloro-sodalite ($Na_4[AlSiO_4]_3Cl$).

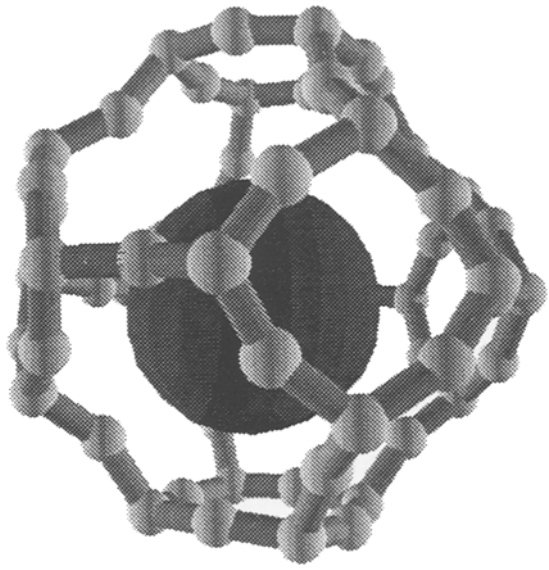

Figure 11. A plot of the electron density for the solvated electron in the ground state in the electron injected dehydrated sodalite ($Na_3[AlSiO_4]_3$).

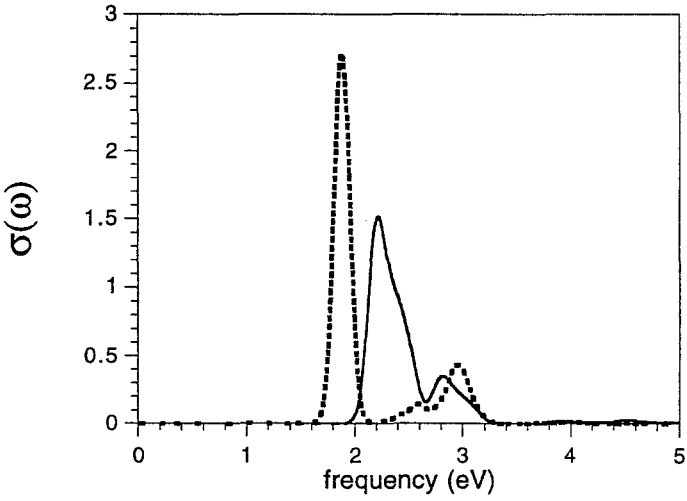

Figure 12. Calculated absorption spectra for Na_3^{2+} in dehydrated sodalite. The dotted line is the spectrum for the cluster in the dipole-aligned crystal, while the solid line is the spectrum for the dipole-misaligned sample.

Recently, this pseudo-potential description of electron solvation has been applied to the Na_3^{2+} cluster within dry sodalite [32]. In particular, we have been interested in the theoretical prediction of the absorption spectrum to see whether of not this is consistent with the assignment of Kerry Thomas' group [3,5]. Theoretically, it is found that introduction of an electron into an otherwise perfect dehydrated sodalite lattice leads to a significant polarization of the system. The Na_3^{2+} contracts substantially on formation of the cluster with the next nearest neighbors sitting at the windows of the cage. The ground state is shown in Figure 11 as with the Na_4^{3+} cluster the electron is delocalised at the center of the cluster occupying the space between the ions - again in agreement with the inferences from EPR coupling constant data. The calculated absorption cross-section is shown in Figure 12. The cross-section exhibits a maximum at 1.7 eV in agreement with experiment.

3.2 SPECTROSCOPIC STUDIES OF AGGREGATED CLUSTERS

When the zeolite is exposed to high concentrations of alkali-metal vapor, it is possible to produce samples where solvated electrons are present in large percentages of the cavities. As we noted above, such solids are typically black or dark brown in color. In black sodalite, for example, XRD shows that each sodalite cage contains an excess Na-ion filling all ionic sites within the sodalite (Srdanov, Monnier et al.). The cell constant contracts considerably from the dehydrated sodalite starting material, changing from 9.1 Å to 8.9 Å, and the Na ions move toward the center of the cage. The optical absorption spectrum lineshape broadens to a continuum with a threshold for absorption at around 0.8 eV.

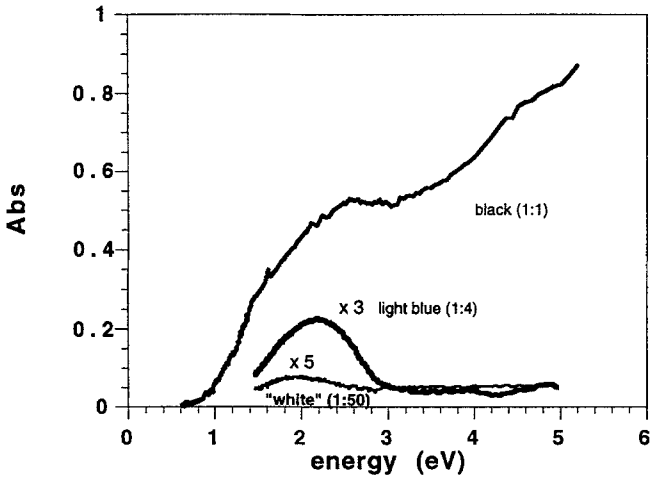

Figure 13. The evolution of the optical absorption spectrum of the Na-doped dehydrated sodalite, (reproduced by kind permission of Dr. V. I. Srdanov).

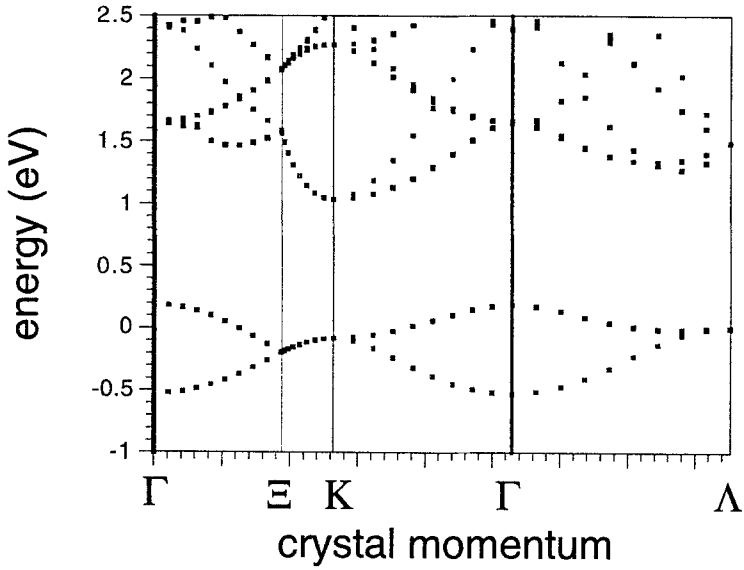

Figure 14. The calculated band structure of black sodalite in the independent electron approximation. There is a total of two electrons per unit cell in black sodalite; therefore, at 0 K, only the lowest band is occupied.

Figure 13 shows how the absorption profile changes as a function of the doping level. From these reflectance studies, it appears that, at high sorption levels, the material is a semiconductor with a band gap of 0.8 eV or so. Recently, improved doping methods lead to a black sodalite phase which exhibits a very narrow EPR singlet resonance (see Figure 4) the width and intensity of which is apparently temperature independent down to 4 K. SQUID measurements of this same material confirm its metallic nature.

In an attempt to rationalize these apparently contradictory observations, Blake et al. [33] have repeated the earlier band-structure calculations of Monnier, Stucky, and Metiu [34], with the same pseudo-potentials used to model the isolated color-center systems as Blake et al. [28]. The band structure is shown in Figure 14. In the absence of band degeneracies, the 2 electrons per unit cell would imply that the material was an insulator at 0 K. However, degeneracy of this valence band with the lowest lying excited band at the edges of the Brillioun zone, as well as along $\{100\}\leftrightarrow\{110\}$, indicate that the crystal is a semi-metal and as such will be weakly ferromagnetic. The joint density of states and the transition probability are shown in Figure 15 along with the experimental band

structure. Firstly, note the reasonably large contribution to the joint density of states at 0 eV indicating a large region of degeneracy between the lowest two bands. Secondly, transitions from the valence band (this band can be considered as a symmetric combination of the Na_4^{3+} orbitals in neighboring cages) to the lowest unoccupied band (the antisymmetric combination of the Na_4^{3+} orbitals in neighboring cages) are forbidden owing to a vanishing matrix element between these Bloch states. The spectrum

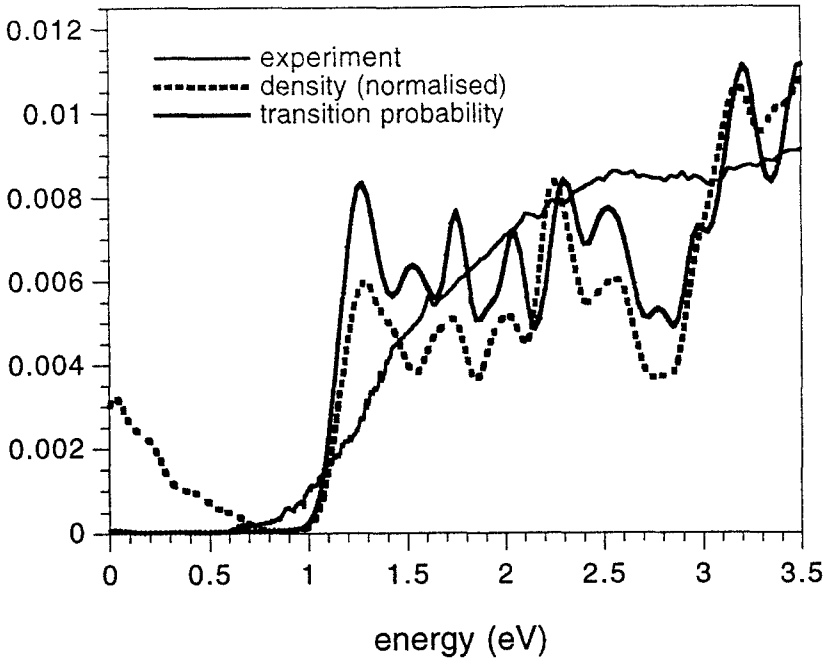

Figure 15. A comparison of the calculated joint density of states: the calculated and observed spectra for black sodalite (after [7]). All calculations are for 0 K while the experimental spectrum is recorded at room temperature.

therefore exhibits an onset for absorption of approximately 1 eV - in reasonable agreement with experiment. The structure in the spectrum corresponds to transitions at the edges of the Brillioun zone. The strongest feature corresponds to vertical transitions at the K and Γ points to the T_2 states at around 2.4 eV, in agreement with experiment. The point of inflexion at around 3 eV corresponds to the gap between the states comprised of the T_2 ("p") states and states comprised of the "d" orbitals of the color center. The calculations, however, predict a much sharper onset for absorption,

suggesting that perhaps the preliminary absorption data are not for 100% black sodalite. This has been confirmed recently through NMR, which estimates the material to be 68% black sodalite. Band structure calculations of $Na_7(AlSiO_4)_6$·e reveal that this onset is lower (0.8 eV) than the fully-doped material [33]. Thus, at this point, it seems likely that the "black" sodalite spectrum is a superposition of these two materials and perhaps even some of the isolated clusters.

EPR of the black phase shows, that as one increases the Na doping levels, the EPR spectrum collapses from the 13-line pattern to a singlet. This observation was first noted by Edwards and Harrison in 1984 [13] in conjunction with Na-X and Na-Y, where the similarity to the spectrum obtained in colloidal Na metal led to a metallic cluster assignment. In the years following this influential work, all observations of such clusters were attributed to metallic Na - even in Na-doped halo-sodalites, where there is no room for such a species! Later, Anderson and Edwards [15] re-assessed the validity of such an assignment - realizing that in all other respects this EPR signal bore little resemblance to a conduction-electron EPR signal, (i.e., no Knight shift, wrong temperature dependence for the line-width, etc.) Careful analysis of the lineshape as a function of the dopant levels showed that the collapse to a singlet occurred at levels where it was statistically likely that solvated electron clusters were present in neighboring cages. They postulated that the singlet signal arose as a result of an exchange mechanism and showed by modeling of the EPR spectrum how reasonable values for the exchange integral led to collapse to a singlet structure with even one neighboring cluster. Thus, the EPR spectrum shows evidence that color centers in neighboring cages are coupled - dashing hopes of using alkali-metal clusters in zeolites to study quantum size effects - where such interactions are normally ignored. These observations are also consistent with the magnetic properties of the less than fully doped black sodalite phase, which exhibits an antiferromagnetic transition at around 60 K [35].

4. Prospects for the Future

In the preceding pages we have brought the reader to the present state of alkali-cluster research in zeolites. To some extent, we have concentrated on the theory of the optical properties of these color centers - reflecting simply our present research interests. We have shown how electron solvation theory is successful in predicting the observed optical behavior of these color centers in sodalites and, at the other extreme how the theory, when used in conjunction with Bloch theory, can qualitatively reproduce the optical behavior of the black phase. The present level of theory is thus helping us to qualify some of the interesting properties exhibited by such alkali-metal clusters. Preliminary results for the K derivatives indicate that these solids may have very different electronic and magnetic properties to the Na derivatives and the understanding of the K-doped sodalites is one of the main thrusts of our group. The characterization of the highly doped solids is, however, the object of many groups' research. In particular, interest is focusing on the possibility of effecting an insulator-metal transition in these systems [36].

Estimates for the faujasites indicate that they are close to obtaining the required 10^{21} electrons cm^{-3} required by the Mott criterion [37] for transition to the metallic phase [36]. Interestingly, the fully doped sodalite fulfills this condition and indications are that, if carefully made, it is metallic.

For the future, it seems certain that careful, temperature-dependent, EPR and SQUID measurements will uncover the mysteries of the highly doped materials and the unique properties conferred on them by the zeolite.

Acknowledgments

We gratefully acknowledge partial funding from O.N.R. and the Center for QUantised Electronic STructures (QUEST). Furthermore, we would like to thank Dr. Vojislav I. Srdanov for both the helpful discussions and for the use of both his EPR and optical absorption data for black sodalite. Finally, we would like to thank Prof. J. Kerry Thomas and Prof. Peter Edwards for kindly granting permission for the reproduction of EPR data.

References

1. P. T. Bolwijn, D. J. Schipper, and C. Z. van Doorn, *J. Appl. Phys.*, **43**, 132 (1972).
2. P. H. Kasai, *J. Chem. Phys.*, **43,** 3322 (1965).
3. K. K. Iu, X. Liu and J. K. Thomas, *J. Phys. Chem.*, **97**, 8165 (1993).
4. (a) P. A. Anderson, D. Barr, and P. P. Edwards, *Angew. Chem. Int. Ed. Engl.*, **30**, 1501 (1991);
   (b) P. A. Anderson and P. P. Edwards, *J. Chem. Soc., Chem. Commun.*, 915 (1991);
   (c) P. A. Anderson, R. J. Dancer, and P. P. Edwards, *J. Chem. Soc., Chem. Commun.*, 914 (1991).
5. X. Liu and J. K. Thomas, *Langmuir*, **8**, 1750 (1992).
6. R. M. Barrer and J. F. Cole, *J. Phys.Chem. Solids*, **29**, 1755 (1968).
7. V. I. Srdanov, K. Haug, H. Metiu, and G.D. Stucky, *J. Phys. Chem.*, **96**, 9039 (1992).
8. J. B. A. F. Smeulders, M. A. Hefni, A. A. K. Klassen, E. de Boer, U. Westphal, and G. Geismar, *Zeolites*, **7**, 347 (1987)
9. G. D. Stucky, L. Iton, T. Morrison, G. Shenoy, S. Suib, and R. P. Zerger, *J. Mol. Catal.*, **27**, 71-80 (1980); *J. Chem. Phys.*, **80**, 2203 (1984).
10. T. L. Barr, L. M. Chen, M. Mohsenian, and M. A. Lishka, *J. Am. Chem. Soc.*, **110**, 7962 (1988).
11. X. Liu, K. K. Iu, and J. K. Thomas, *Chem. Phys. Lett.*, **224**, 31 (1994).
12. J. A. Rabo, C. L. Angell, P. H. Kasai and V. Schomaker, *Discuss. Faraday Soc.*, **41**, 328 (1966)

13. P. P. Edwards, M. R. Harrison, J. Klinowski, S. Ramdas, J. M. Thomas, D. C. Johnson, and C. J. Page, *J. Chem. Soc., Chem. Commun.*, 982 (1984)
14. J. Dye, *J. Phys. Chem.*, **84**, 1084 (1980)
15. P. A. Anderson and P. P. Edwards, *J. Am. Chem. Soc.*, **114**, 10608 (1992).
16. T. Sun and K. Seff, *J. Phys. Chem.*, **98**, 10156 (1994).
17. P. A. Anderson, R. J. Singer, and P. P. Edwards, *J. Chem. Soc., Chem. Commun.*, 914 (1994).
18. A. Stein, P. M. Macdonald, G. A. Ozin, and G. D. Stucky, *J. Phys. Chem.*, **94**, 6943 (1990).
19. R. Jelinek, B. F. Chmelka, A. Stein, and G. A. Ozin, *J. Phys. Chem.*, **96**, 6744-6752 (1992)
20. S. H. Song, Y. Kim, and K. Seff *J. Am Chem. Soc.*, **97**, 10139 (1993);
N. H. Heo and K. Seff, *J. Am. Chem. Soc.*, **109**, 7986 (1987); *J. Chem. Soc., Chem. Commun.*, 1225 (1987); *Zeolites*, **12**, 819 (1992);
N. H. Heo, C. Dejsupa, and K. Seff, *J. Phys. Chem.*, **91**, 3943 (1987); *Zeolites*, **9**, 146 (1989).
21. S. H. Song, U. S. Kim, Y. Kim, and K. Seff, *J. Phys. Chem.*, **96**, 10937 (1992).
22. S. H. Song , Y. Kim, and K. Seff, *J. Phys. Chem.*, **95**, 9919 (1991).
23. K. K. Iu and J. K. Thomas, *J. Phys. Chem.*, **95**, 506 (1991); *Colloids Surf.*, **63**, 39 (1992).
24. K. B. Yoon and J. K. Kochi, *J. Chem. Soc., Chem. Commun.*, 510 (1988).
25. L. R. M. Matens, P. J. Grobet, and P. A. Jacobs, *Nature*, **315**, 568 (1985).
26. B. Xu, X. Chen, and L. Kevan , *J. Chem. Soc., Faraday Trans.*, **87**, 3157 (1991).
27. K. Haug, V. I. Srdanov, G. D. Stucky, and H. Metiu, *J. Chem. Phys.*, **96**, 3495 (1992).
28. N. P. Blake, V. Srdanov, G. D. Stucky, and H. Metiu, *J. Phys. Chem., in press.*
29. P. Sen, C. N. R. Rao, and J. M. Thomas, *J. Mol. Struct.*, **146**, 1711 (1986).
30. R. D. Shannon, *Acta Crystallogr.*, **A32**, 751 (1976).
31. N. P. Blake and H. Metiu, *J. Chem. Phys., submitted.*
32. N. P. Blake and H. Metiu, *J. Phys. Chem, to be submitted.*
33. N. P. Blake, V. I. Srdanov, G. D. Stucky, and H. Metiu, *Phys. Rev. Lett., to be submitted.*
34. A. Monnier, G. D. Stucky, and H. Metiu, *J. Chem. Phys.*, **100**, 6944 (1994).
35. V. I. Srdanov and G. D. Stucky, *in preparation.*
36. P. P. Edwards, L. J. Woodhall, P. A. Anderson, A. R. Armstrong, and M. Slaski, *Chem. Revs.*, 305 (1993).
37. P. P. Edwards and M. J. Sienko, *J. Am. Chem. Soc.*, **103**, 2697 (1981).

Abstract. Zeolites are unique in that they can play host to a large number of alkali-metal clusters of the type M_n^{+p} hitherto unseen in any other system. When isolated, these clusters behave as color centers. The alkali ions reside in ionic sites within the cavities and so the nature of the cluster is very much a function of the zeolite host, the Si:Al ratio, and the method chosen to prepare the cluster. Since these centers are created within zeolite cages rather than as structural defects (as is the case with the alkali halides) high cluster concentrations can be achieved at which point the optical and magnetic properties of the zeolite change profoundly. We review experimental work in this area, as well as our own attempts to understand both the electronic and optical properties of these systems in terms of an electron solvation model.